

DOI: 10.1002/chem.201201840

Experimental Study of Hydrogen Bonding Potentially Stabilizing the 5'-Deoxyadenosyl Radical from Coenzyme B₁₂Peter Friedrich,^[a, b] Ulrich Baisch,^[a] Ross W. Harrington,^[a] Fredrick Lyatuu,^[b] Kai Zhou,^[c] Felix Zelder,^[c] William McFarlane,^[a] Wolfgang Buckel,^[b, d] and Bernard T. Golding*^[a]

Dedicated to Professors Duilio Arigoni and János Rétey

Abstract: Coenzyme B₁₂ can assist radical enzymes that accomplish the vicinal interchange of a hydrogen atom with a functional group. It has been proposed that the Co–C bond homolysis of coenzyme B₁₂ to cob(II)alamin and the 5'-deoxyadenosyl radical is aided by hydrogen bonding of the corrin C19–H to the 3'-O of the ribose moiety of the incipient 5'-deoxyadenosyl radical, which is stabilized by 30 kJ mol⁻¹ (B. Durbeej et al., *Chem. Eur. J.* **2009**, *15*, 8578–8585). The diastereoisomers (*R*)- and (*S*)-2,3-dihydroxypropylcobalamin were used as models for coenzyme B₁₂. A downfield shift of the NMR signal for the C19–H proton was observed for the (*R*)-isomer ($\delta = 4.45$ versus 4.01 ppm for the (*S*)-isomer) and can be ascribed to an intramolecular hydrogen bond between the C19–H and the

oxygen of CHOH. Crystal structures of (*R*)- and (*S*)-2,3-dihydroxypropylcobalamin showed C19–H...O distances of 3.214(7) Å (*R*-isomer) and 3.281(11) Å (*S*-isomer), which suggest weak hydrogen-bond interactions ($-\Delta G < 6$ kJ mol⁻¹) between the CHOH of the dihydroxypropyl ligand and the C19–H. Exchange of the C19–H, which is dependent on the cobalt redox state, was investigated with cob(I)alamin, cob(II)alamin, and cob(III)alamin by using NMR spectroscopy to monitor the uptake of deuterium from deuterated water in the pH range 3–11. No exchange was found for any of the cobalt

oxidation states. 3',5'-Dideoxyadenosylcobalamin, but not the 2',5'-isomer, was found to act as a coenzyme for glutamate mutase, with a 15-fold lower k_{cat}/K_M than 5'-deoxyadenosylcobalamin. This indicates that stabilization of the 5'-deoxyadenosyl radical by a hydrogen bond that involves the C19–H and the 3'-OH group of the cofactor is, at most, 7 kJ mol⁻¹ ($-\Delta G$). Examination of the crystal structure of glutamate mutase revealed additional stabilizing factors: hydrogen bonds between both the 2'-OH and 3'-OH groups and glutamate 330. The actual strength of a hydrogen bond between the C19–H and the 3'-O of the ribose moiety of the 5'-deoxyadenosyl group is concluded not to exceed 6 kJ mol⁻¹ ($-\Delta G$).

Keywords: coenzyme B₁₂ • 5'-deoxyadenosyl radical • enzymes • hydrogen bonds • mutase • radical ions

Introduction

Coenzyme B₁₂-dependent enzymes comprise of mutases, which catalyze either carbon-skeleton rearrangements or 1,2-shifts of amino groups, and eliminases, which bring about the loss of ammonia or water from a substrate molecule^[1] and include class II ribonucleotide reductase.^[1e,2] The catalytic activity of coenzyme B₁₂-dependent enzymes depends on homolytic cleavage of the relatively weak cobalt(III)–carbon σ -bond (bond dissociation energy ≈ 130 kJ mol⁻¹)^[3] to provide cob(II)alamin and the 5'-deoxyadenosyl (Ado) radical. The primary organic Ado radical abstracts a hydrogen atom from the substrate to form 5'-deoxyadenosine and a substrate-derived radical, which rearranges to a form a product-related radical. Abstraction of a hydrogen atom from the methyl group of 5'-deoxyadenosine by the product-related radical then gives the product with regeneration of the Ado radical.^[1d,h,4] Among the important unresolved issues with this pathway are how the Co–C bond homolysis is achieved at a rate appropriate for the enzymat-

[a] Dr. P. Friedrich, Dr. U. Baisch, Dr. R. W. Harrington, Prof. Dr. W. McFarlane, Prof. Dr. B. T. Golding
School of Chemistry, Newcastle University
Newcastle upon Tyne, NE1 7RU (UK)
E-mail: bernard.golding@newcastle.ac.uk

[b] Dr. P. Friedrich, F. Lyatuu, Prof. Dr. W. Buckel
Laboratorium für Mikrobiologie, Fachbereich Biologie
Philipps-Universität, 35032 Marburg (Germany)

[c] K. Zhou, Dr. F. Zelder
Institute of Inorganic Chemistry, University of Zürich
Winterthurerstrasse 190, 8057, Zürich (Switzerland)

[d] Prof. Dr. W. Buckel
Max-Planck-Institut für terrestrische Mikrobiologie
Karl-von-Frisch-Str. 10, 35043 Marburg (Germany)

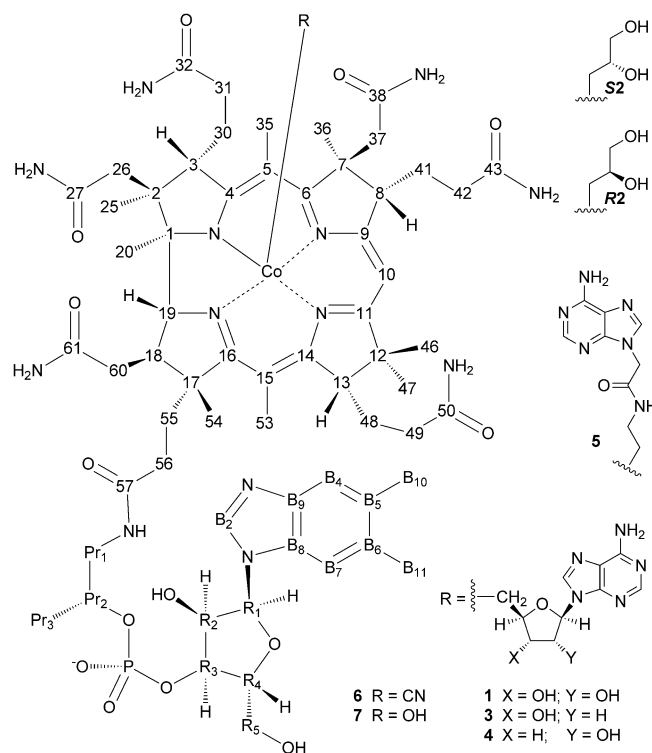
Supporting information for this article is available on the WWW under <http://dx.doi.org/10.1002/chem.201201840>.

ic processes and whether the intermediate radicals are stabilized by cob(II)alamin.^[1e]

For mutases (e.g., glutamate mutase), it has been proposed that cob(II)alamin stabilizes the intermediate methylene radicals, thus acting as a so-called conductor and lowering the transition-state energy barrier for radical formation and rearrangement.^[1e] The energy difference between a concerted mechanism for the formation of a substrate-derived radical that is stabilized by cob(II)alamin (i.e., conductor) and a stepwise reaction sequence with cob(II)alamin as a spectator was calculated to favor the former by about 30 kJ mol⁻¹.^[5] For the eliminases, cob(II)alamin is a spectator to the rearrangement step.^[6] There are also some eliminases in which coenzyme B₁₂ is replaced by *S*-adenosylmethionine (SAM), a source of the 5'-deoxyadenosyl radical but not of cob(II)alamin, for example, class III ribonucleotide reductase from *Escherichia coli* or bacteriophage T4 and glycerol dehydratase from *Clostridium butyricum*.^[2,7] The conductor–spectator subdivision is in accord with EPR studies and protein crystallography. EPR spectroscopy showed that the distance between cob(II)alamin and an intermediate radical is about 10 Å in the eliminases, for example, ethanolamine ammonia lyase (EAL).^[8] The crystal structures of EAL^[9] and diol dehydratase^[10] showed a similar distance from the cobalamin to the bound substrate. However, according to EPR data^[11] and protein crystallography^[12] for the mutases, the distance between cob(II)alamin and a bound substrate-derived radical is about 6 Å. The EPR spectra demonstrated an interaction between the two radicals, albeit a very weak one.^[11b]

The application of density functional theory by using ribosylcobalamin as a model for coenzyme B₁₂ led to the proposal of a hydrogen bond between the 3'-oxygen atom of the ribose moiety and the cobalamin C19–H (protons are designated according to the system of Marzilli et al.;^[13] Scheme 1). This interaction was supposed to stabilize the ribosyl methylene radical/cob(II)alamin pair.^[14] After fission of the Co–C bond, pseudorotation of the ribose from the C2'-endo to C3'-endo conformation^[12b] was required to bring the 3'-OH into a suitable position (3.5 Å distance; 5.3 Å without the conformational change) to interact with the C19–H. The degree of stabilization was calculated to be about 30 kJ mol⁻¹ and was proposed to contribute to the lowering of the transition state energy for hydrogen atom abstraction from a substrate molecule (e.g., glutamate).^[14] Furthermore, the Co atom of cob(II)alamin was deemed important for enhancing the polarization of the C19–H bond through the intervening nitrogen atom, thus facilitating hydrogen bonding with 3'-OH.

The putative interaction of the C19–H with the 3'-oxygen of Ado is an example of a C–H donor to an O acceptor hydrogen bond,^[15] classically defined by the chloroform donor–acetone acceptor system.^[16] Recently studied examples include the interaction of a hydroxyl group with a neighboring methyl group^[17] and a glutamine (amide CO) residue that hydrogen bonds (2.0 Å) to a histidine C–H.^[18] Hydrogen bonds between a C–H donor and an O acceptor



Scheme 1. Alkylcobalamins (**R2**, **S2**, **3–5**) obtained from cyanocobalamin (CNCbl, R = CN, **6**) by using chlorinated adenine precursors; hydroxocobalamin (HOCbl, R = OH, **7**). Numbering system for cobalamin protons is adapted from that of Calafat and Marzilli.^[13]

are generally weaker ($\Delta G \approx 2\text{--}5 \text{ kJ mol}^{-1}$)^[18] than those in which an OH or NH group acts as a donor to the C=O oxygen ($\Delta G \approx 15 \text{ kJ mol}^{-1}$), although the ΔG values for hydrogen bond formation depend strongly on the environment (gas, liquid, or solid phase).^[15]

A study of the diastereoisomers (*R*)- and (*S*)-2,3-dihydroxypropylcobalamin (**R2** and **S2**, respectively) by NMR spectroscopy revealed a surprising downfield shift of the C19–H proton for the (*R*)-isomer (4.60 ppm versus 4.17 ppm for the (*S*)-isomer).^[19] These are model compounds for coenzyme B₁₂, with the (*S*)-isomer exactly overlaying the structure of the coenzyme. One aspect of the present study was to investigate the possibility that the difference in chemical shift of the signal for the C19–H in **R2** compared to **S2** is due to a specific hydrogen bond between the C19–H and the 2'- or 3'-O of **R2**. This question has been addressed by searching for coupling between the C19–H and protons in the dihydroxypropyl group. The detection of hydrogen bonding between an oxygen of **R2** and/or **S2** and the C19–H would indicate that, in principle, this type of interaction is possible for the 3'-O of the Ado radical that is formed by homolysis of the Co–C bond of coenzyme B₁₂. During an attempt to redetermine the crystal structures of **R2** and **S2** at a higher resolution than previously reported^[20] to enable the detection of hydrogen bonds, new crystal forms of **R2** and **S2** were discovered and a better insight into the geometry and hydrogen-bond interactions of these compounds was ob-

tained. In another aspect of this study, exchange of the C19–H with solvent protons, which is dependent on the cobalt redox state, was investigated. Finally, the cofactor properties of 2',5'-dideoxyadenosyl- (**3**) and 3',5'-dideoxyadenosyl-cobalamin (**4**), in which the 2'- and 3'-OH groups have been deleted in turn, and of peptidoadenylcobalamin (**5**) have been determined. Thus, four complementary experimental techniques have been used to probe the reality or otherwise of hydrogen bonding between C19–H and a neighboring hydroxyl group.

The complementary studies described in this paper show that although there is experimental support for weak hydrogen bonding ($\Delta G < 6 \text{ kJ mol}^{-1}$) between the C19–H of a cobalamin and a hydroxyl substituent on a cobalt–alkyl group, the polarization of the C19–H is insufficient to enable its exchange with solvent protons in any cobalamin oxidation state. The 15-fold reduced ability of 3',5'-dideoxyadenosyl-cobalamin (**4**) to act as a coenzyme with glutamate mutase compared with coenzyme B₁₂ corresponds to a change in transition state energy of 7 kJ mol^{-1} , which may be due, in part, to the loss of the C19–H/Ado interaction.

Results and Discussion

(R)- and (S)-2,3-Dihydroxypropylcobalamin: These compounds (designated as **R2** and **S2**) are models for coenzyme B₁₂ (**1**; note that the configuration at C4' in coenzyme B₁₂ corresponds to that of the dihydroxypropyl group of **S2**) and exhibit a surprising difference in the chemical shift of the C19–H signal in their ¹H NMR spectra. Experimental values for **R2** and **S2** are 4.45 ppm and 4.01 ppm, respectively (Figure 1), and literature values are^[19] 4.60 ppm and

4.17 ppm, respectively. This observation could be interpreted as evidence for a hydrogen bond between the C19–H and one of the propyl hydroxyl groups of **R2**. To obtain further evidence, additional NMR experiments on **R2** and **S2** were undertaken.

Neither two-dimensional (2D) nuclear Overhauser effect spectroscopy (NOESY) nor 2D rotating-frame Overhauser effect spectroscopy (ROESY) showed any NOE between the C19–H and protons of the 2,3-dihydroxypropyl group. Double-pulsed field gradient spin-echo 1D NOE and ROE experiments^[21] also failed to detect NOE interactions involving the C19–H and the 2,3-dihydroxypropyl ligand. Field gradient HMBC experiments showed no scalar coupling between the C19–H and ¹³C nuclei in the 2,3-dihydroxypropyl group, or between ¹³C19 and protons of the 2,3-dihydroxypropyl group.

R2 and **S2** crystallized in different forms (designated **R2b** and **S2b**) compared to the crystal structures reported previously (**R2a** and **S2a**).^[20] Different unit-cell dimensions and numbers of disordered solvent molecules were observed for the new structures. Because of the high positional disorder of water and acetone in the cavities between cobalamin molecules, the resolution of these structures was not as high as expected and the statistics are only slightly better than those reported previously.^[20] The major difference between **S2a** and **S2b** lies in the orientation of the dihydroxypropyl ligand. In both structures, water molecules surround this fragment and engage in hydrogen bonding. In **S2a**, no hydrogen bond is present between the C19–H and the CHOH group of the dihydroxypropyl ligand (distance > 4 Å); however, **S2b** shows a weak hydrogen bond of 3.281(11) Å between the C19–H and the CHOH, which is facilitated by rotation of the ligand around its axis (Figure 2).

Surprisingly, **R2a** and **R2b** exhibited different intermolecular interactions, in particular between the dihydroxypropyl and acceptor groups of the adjacent molecule. In **R2b**, the OH groups of the dihydroxypropyl ligand show hydrogen bonding to one phosphate oxygen (O4a(H)⋯O2P = 2.738(6) Å) as well as further interactions to the N(59)H group attached to carbon PR1 and C57, and to one acetamide carbonyl (C61=O62). In **R2a**, no hydrogen bonding is observed, with only solvent water molecules acting as hydrogen-bond acceptors. The C19⋯O distances are 3.29(3) Å for **R2a** and 3.214(7) Å for **R2b**, which imply that a weak C19–H⋯O interaction with one of the propyl hydroxyl groups is pres-

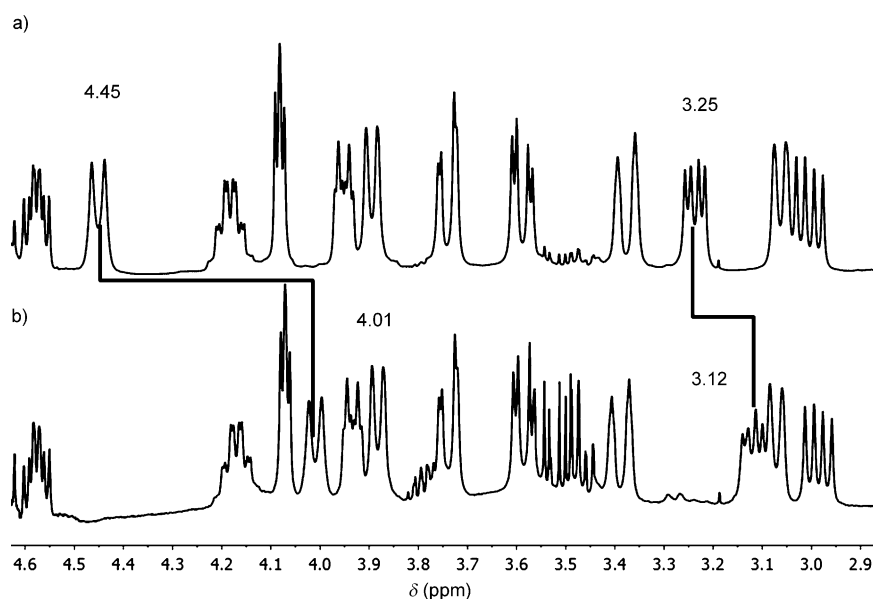


Figure 1. ¹H NMR (400 MHz, in D₂O) spectra of a) (R)- and b) (S)-2,3-dihydroxypropylcobalamin (**R2**, **S2**). Chemical shifts of the C19–H and C8–H are indicated.

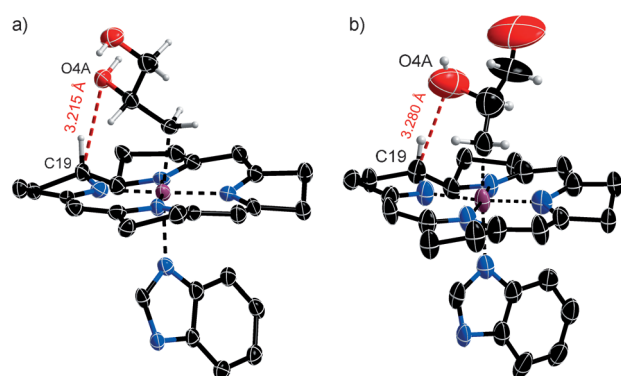


Figure 2. Fragments of the crystal structures of a) **R2b** and b) **S2b**. Thermal ellipsoids are depicted at a 50% probability level.

ent in each structure. For lists of the hydrogen-bond interactions, bond distances, and angles, see the Supporting Information.

Exchange of cobalamin protons dependent on cobalt oxidation state:

Cob(III)alamin, cob(II)-alamin, and cob(I)alamin were examined for the exchange of C19–H and other protons in the pH range 3.0–10.8 (see the Supporting Information, Figure S3). Note that hydroxocobalamin (**7**, cob(III)alamin state) is protonated to aquocobalamin ($pK_a \approx 7.3$ – 8.1 at 25°C) at $\text{pH} < 7$, and many of the resonances that arise from C–H bonds, for example, B2–H and C10–H, shift in response to the pH of the sample (see the Supporting Information, Figure S2, left arrows). It is assumed that the NMR spectra

show aquocobalamin at pH 6, and hydroxocobalamin at pH 9. Compound **7** was reduced to cob(II)alamin by dithiothreitol (DTT) or PtO_2/H_2 . Light-driven homolytic cleavage of 5'-deoxyadenosylcobalamin (**1**) was also employed to generate cob(II)alamin. Cob(I)alamin was obtained by the reduction of **7** with sodium dithionite.^[22] The typical UV/Vis absorption maxima at around $\lambda_{\text{max}} = 550$ nm for cob(III)alamin and 460 nm for cob(II)alamin vanished after reduction to cob(I)alamin. The known cob(II)alamin EPR signal was obtained only after reduction by PtO_2/H_2 or DTT. The control sample of untreated **7** and the dithionite-reduced sample displayed no EPR signal. After conducting an exchange experiment, the samples were reoxidized by air to **7** prior to analysis, except for the DTT reductions and kinetic studies with short incubation times, which required oxidation by potassium hexacyanoferrate(III). Deuterium that remained in readily exchangeable positions (OD and ND) was

removed by freeze-drying after equilibration in H_2O . MALDI-TOF-MS and 1D- and 2D-NMR spectroscopy were used to analyse the samples for exchanged hydrogen atoms (see the Supporting Information for full details). Within experimental error, the NMR integrals matched the MALDI-TOF-MS analysis of the samples.

The ^1H NMR chemical shifts assigned for previous B₁₂ derivatives^[1b,13,19,23] assisted the data analysis given here. As a control, **7** was incubated in D_2O for up to one week at 20°C with pH values of 3, 6, 7, 8, and 10.8 without significant exchange of the C19–H, C10–H, B2–H, or any other CH proton being observed (see the Supporting Information, Figures S2 and S3). C10–H was reported to exchange at a strongly acidic pH,^[24] but at pH 3, no significant exchange was visible (Figure 3 (bottom) and Figure S2 in the Supporting Information).

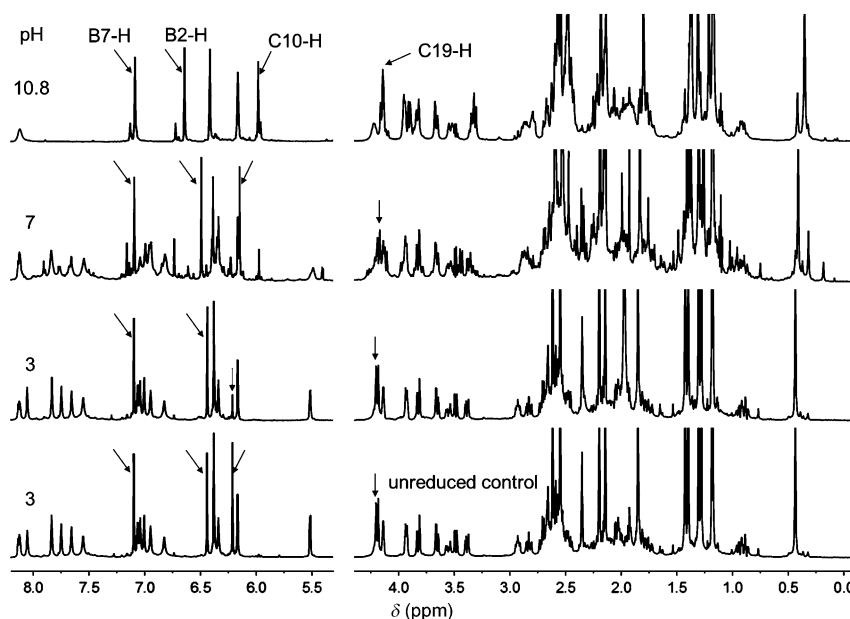


Figure 3. The exchange of cob(II)alamin (from the reduction of **7** with PtO_2/H_2) in D_2O at pH 3, 7, and 10.8 as monitored by 600 MHz ^1H NMR. The water signal is omitted.

Similar experiments with cob(II)alamin showed exchange for C10–H to occur primarily at pH 3 (Figure 3), which was limited to the incorporation of a single deuterium atom at values up to pH 6 (see the Supporting Information, Figures S1, S4, S6, and S8). Exchange at pH 10.8 (see the Supporting Information, Figures S1 and S5) could not be attributed to a single position and is due to side reactions at elevated pH (see the Supporting Information). The C19–H doublet was clearly visible in one-dimensional NMR and ^1H - ^1H -DFQ-COSY spectra showed the known correlation network to C18–H and C60–H, regardless of pH, without any significant decrease in the C19–H peak intensity compared to the cob(III)alamin control (see the Supporting Information, Figure S3).

Cob(I)alamin showed exchange at every pH level tested (see the Supporting Information, Figures S1 and S9) and could be attributed to two positions: C10–H (predominant

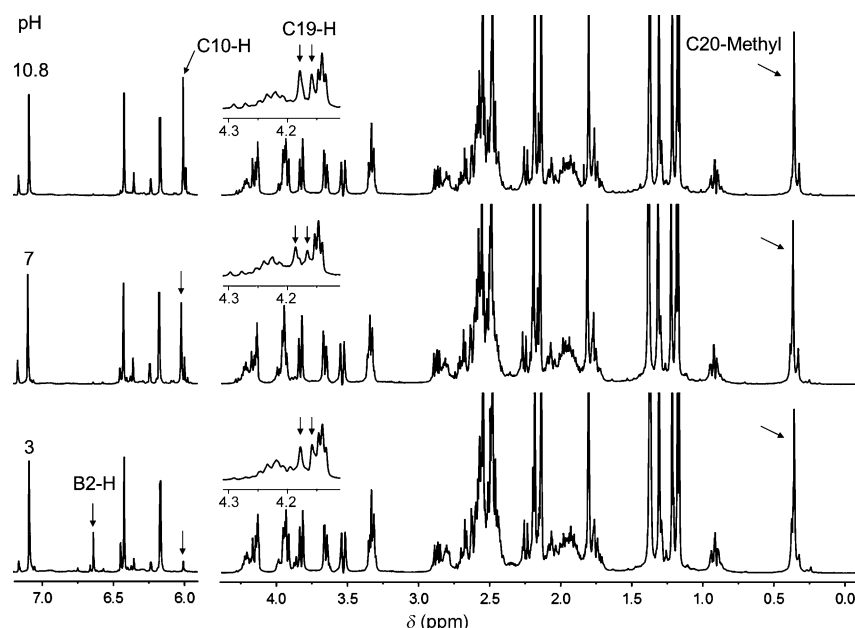


Figure 4. The exchange of cob(I)alamin (from the reduction of **7** with dithionite) in D₂O at pH 3, 7, and 10.8 as monitored by 600 MHz ¹H NMR at pH 9. Highlighted resonances: C19–H (broad doublet); C10–H (s; δ = 6.00 ppm); B2–H (s, δ = 6.63 ppm). The water signal is omitted.

at pH 3) and B2–H (complete at pH 7 and 10.8, Figure 4). The C19–H doublet (δ = 4.2 ppm) was clearly visible in one dimensional ¹H NMR (Figure 4).

Kinetic and binding studies of glutamate mutase with cobalamin derivatives: To investigate the role of the 3'-hydroxyl group of the 5'-deoxyadenosyl moiety of coenzyme B₁₂ (**1**) during the reaction of glutamate mutase, 2',5'-dideoxyadenosyl- (**3**), 3',5'-dideoxyadenosyl- (**4**), and peptidoadenyl-cob-

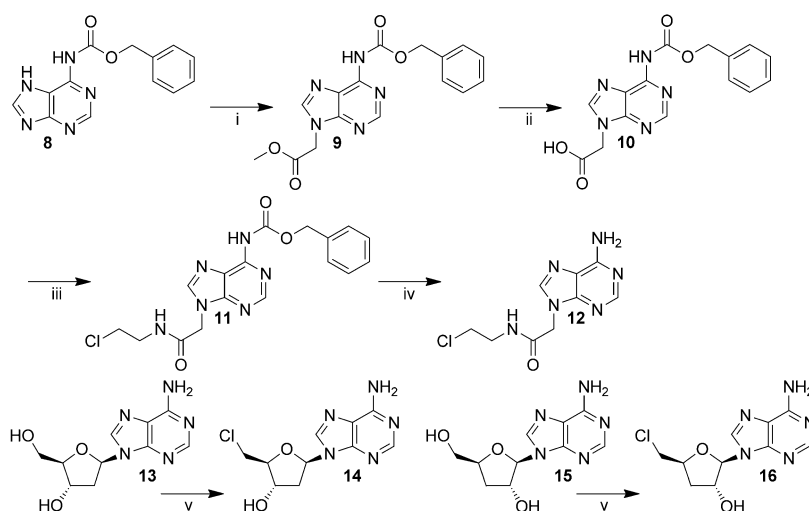
alamin (**5**) were synthesized (see Scheme 2) and tested along with HOCbl (**7**). Compounds **1** and **4** exhibited similar affinities for the enzyme (compare the apparent K_M values: **1** $0.52 \pm 0.06 \mu\text{M}$; **4** $0.56 \pm 0.02 \mu\text{M}$). However, **4** showed a 15-fold lower catalytic efficiency ($k_{\text{cat}} = 0.089 \pm 0.01 \text{ s}^{-1}$ and $k_{\text{cat}}K_M^{-1} = 1.59 \times 10^5 \text{ s}^{-1} \text{ M}^{-1}$) than **1** ($k_{\text{cat}} = 1.24 \pm 0.36 \text{ s}^{-1}$ and $k_{\text{cat}}K_M^{-1} = 2.38 \times 10^6 \text{ s}^{-1} \text{ M}^{-1}$) when a 14-fold excess of component S over E was used. No catalytic activity was detected when the holo-glutamate mutase was assembled by using **3** or **5**. The subsequent addition of **1** to the holoenzyme that was assembled with **3** or **5** did not restore the catalytic activity, indicating relatively strong binding of these artificial cofactors to glutamate mutase. HOCbl (**7**)

also assembled the holoenzyme and thus inhibited enzyme activity in a similar fashion.

2,3-Dihydroxypropylcobalamins: (*R*)- and (*S*)-2,3-dihydroxypropylcobalamins (**R2**, **S2**) were used as models for 5'-deoxyadenosylcobalamin (**1**) in experiments to probe for spatial interactions of the C19–H. Neither 1D- and 2D-NMR experiments based on the NOE, nor HMBC experiments, showed spatial interactions of the C19–H with the upper

ligand of **R2** or **S2**. The failure of these measurements to provide evidence for hydrogen bonding between the C19–H and a hydroxyl group may be a consequence of the weakness of the interaction that is indicated by the other approaches described in this paper.

Crystal structures of **R2** and **S2** (except the reported form of **S2a**)^[20] show C19–H...O2 distances that suggest weak hydrogen bond interactions between the dihydroxypropyl ligand and the C19–H. Bond-dissociation energies for these hydrogen bonds are estimated as less than 6 kJ mol^{-1} ,^[15,25] with the distances lying in the predicted range of 3.3 to 3.5 Å. In the crystal form of **S2a**, hydrogen bonding of the dihydroxypropyl



Scheme 2. Synthesis of adenine derivatives. Reagents and conditions: i) Cs₂CO₃, K₂CO₃, methyl bromoacetate, DMF, 2.5 h at RT; ii) aqueous KOH, MeOH, H₂O, 45 min at RT; iii) 2-chloroethanamine hydrochloride, DMF, 4-dimethylaminopyridine (DMAP), 5 min at 0°C followed by 1-ethyl-3-(3-dimethylaminopropyl) carbodiimide (EDC)·HCl, 6 h at RT; iv) Pd on charcoal, H₂, MeOH, 1.5 h at 65°C; v) 1,3-dimethyl-3,4,5,6-tetrahydro-2(1*H*)-pyrimidinone (DMPU), thionyl chloride, 7 h at 0°C.

ligand with the acetamide group of ring B of the next cobalamin molecule is pronounced, whereas the CHO groups in **R2a**, **R2b**, and **S2b** are positioned towards the C19–H.^[20] Both **R2b** and **S2b** show very similar geometrical parameters around the metal atom, and no significant difference in intramolecular interactions were observed between the two diastereoisomers. However, there are significant differences in intermolecular interactions between neighboring cobalamin molecules.

The energy calculations reported by Durbeej et al. assumed a Co–C distance between 3.200 and 4.492 Å to simulate an intermediate state shortly before complete Co–C bond rupture.^[14] This is in sharp contrast to the much shorter bond and therefore more rigid situation that exists in the solid state for **R2** and **S2**. However, it has been shown that weak CH···O interactions do exist for both **R2** and **S2**, but 1) they are subject to different packing variations in the solid, which are primarily directed by intermolecular interactions, and 2) there is only a relatively small gain in the energy associated with the interaction. It is interesting that in all four crystal structures (**R2a**, **R2b**, **S2a**, **S2b**) the dihydroxypropyl ligand has a different orientation. There is enough space for a certain degree of freedom as to how this ligand and its OH groups can be oriented when the compound crystallizes. This can be seen particularly for **S2b**, in which the ligand is rotated about 180° compared to **S2a**. As a consequence, intramolecular hydrogen bonding can now take place. The freedom of orientation of the ligand when it is fully coordinated to the Co centre (1.95–2.07 Å) suggests that when the Co–C distance increases, as in the catalytic cycle of a mutase, then an OH group could adopt a better geometrical arrangement and hence form a stronger hydrogen bond to the C19–H.

Exchange phenomena for cobalamin oxidation states: The NMR (Figures 3 and 4) and mass spectrometric data (see the Supplementary Information) presented in this paper show a sharp distinction in exchange behavior between the three cobalamin oxidation states, with a pH influence present in all cases. For cob(III)alamin, no exchange was observed in the pH range of 3–10.8. For cob(II)alamin, we observed C10–H exchange even in the pH range 3–6, with an increase in rate at lower pH. This behavior can be ascribed to the higher electron density in the corrin ring, which enhances the propensity for protonation at C10. This phenomenon was also observed for cob(I)alamin. In addition, exchange at B2 occurs with a faster rate at higher pH. The mechanism of this exchange probably requires dissociation of the 5,6-dimethylben-

zimidazole from cobalt, followed by a base-mediated reversible deprotonation at B2. The dissociation is facilitated because in cob(I)alamin the cobalt is predominantly in the four-coordinated base-off state.^[26] Despite an extensive search, there was no detectable exchange at the C19–H. Durbeej et al.^[14] suggested that a difference in the electron density of the corrin ring might be able to influence the polarization of the C19–H.^[5] The carbanion that is derived from the deprotonation of the C19–H is expected to be stabilized by delocalization into the corrin π -system. Intuitively, it seems unlikely that an increase in electron density by the reduction of cob(III)alamin to cob(II)alamin or cob(I)alamin could significantly lower the pK_a of the C19–H. Based on our observations, the pK_a of the C19–H is likely to be higher than that of carbon acids such as chloroform (pK_a 21) or even fluoroform (pK_a 27), both of which undergo exchange in alkaline deuterium oxide.^[27]

Biochemical experiments: The strength of the binding of cofactor analogues 2',5'-dideoxyadenosyl- (**3**) and 3',5'-dideoxyadenosyl-cobalamin (**4**) to glutamate mutase was found to be comparable to that of 5'-deoxyadenosylcobalamin (**1**), suggesting that the ribose moiety of the 5'-deoxyadenosyl ligand does not play a major role in cofactor binding. The difference in catalytic efficiency between **4** and **1** converts into a maximum stabilization of the Ado radical by the ribose 3'-OH (7 kJ mol⁻¹) during substrate activation.^[14,28]

An additional, hitherto unrecognized, factor in the stabilization of the Ado radical could be due to an interaction of the 2'-OH of ribose, because compound **3** and peptidoadenylcobalamin (**5**) failed to produce the active holoenzyme. The crystal structure of glutamate mutase^[12b] (Figure 5) reveals the possibility of a hydrogen bond between the 2'-OH and 3'-OH groups with glutamate 330, which could occur before and after homolysis of the Co–C bond. These interactions could act as stabilizing elements for pseudorotation, lowering the energy barrier for radical generation upon substrate addition. Similar conclusions regarding the joint roles

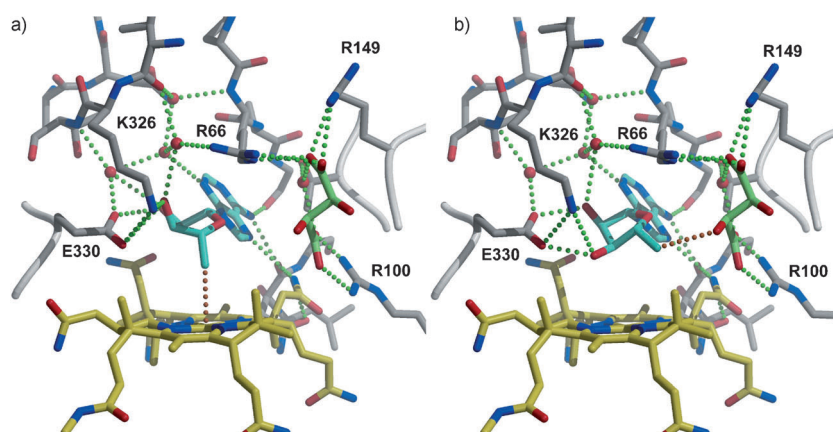


Figure 5. Substrate activation at glutamate mutase active site: a) Co–C bond intact; b) Ado radical is formed and abstracts a substrate hydrogen. Note that pseudorotation of the ribose after Co–C bond cleavage positions ribose 3'-OH within a hydrogen-bonding distance of the C19–H and E330, which can engage in an additional hydrogen bond with the ribose 2'-OH before and after 5'-deoxyadenosylcobalamin homolysis.

of ribose 2'-OH and 3'-OH have been reached based on computational studies with methylmalonyl-CoA mutase^[28] and glutamate mutase (interactions with ribose were tested for K326, E330, and an amide side chain of the corrin ring).^[29] Previous experiments with methylmalonyl-CoA mutase in the presence of 2',5'-dideoxy-adenosylcobalamin (**3**) showed only 1–2% residual activity.^[30]

Conclusion

The experiments presented in this paper detected a weak interaction between the C19-H and a hydroxyl group of the cobalt-bound 2,3-dihydroxypropyl group in **R2** or **S2**, but failed to find exchange of the C19-H in the pH range 3–10.8 for cobalamin in any oxidation state. However, the results demonstrate the influence of the redox state of the cobalt atom in cobalamins on the lower ligand (base-mediated exchange of the B2-H in cob(II)alamin) and the electron density in the corrin ring (exchange by reversible protonation at C10-H for cob(II)alamin and cob(I)alamin).

The experiments with 2',5'-dideoxyadenosylcobalamin (**3**), 3',5'-dideoxyadenosylcobalamin (**4**), and peptidocobalamin (**5**) indicate how the 2'-OH and 3'-OH of the ribose moiety may assist in the generation of the Ado radical and hydrogen abstraction from the substrate. Experimental evidence has been obtained that shows that the 3'-OH group of the ribose could stabilize the Ado radical by a hydrogen bond with the C19-H of cob(II)alamin. However, the experimental estimate for the strength of this hydrogen bond ($\Delta G \approx 6 \text{ kJ mol}^{-1}$) is significantly less than that calculated previously.^[14,28] Hence, the proposal by Durbeej et al.^[14] that cob(II)alamin acts as a conductor through a C19-H hydrogen bond to the 3'-OH of Ado is barely supported. Based on measurements of the activities of **3** and **4** relative to 5'-deoxyadenosylcobalamin, it is suggested that the Ado radical also benefits from an interaction between the ribose 2'-OH and 3'-OH and the glutamate 330 of glutamate mutase. Our conclusions regarding the symbiotic role of the 2'-OH and 3'-OH are consistent with new computational studies.^[28,29]

The question of whether there is any stabilizing orbital interaction between cob(II)alamin and intermediate radicals in mutase reactions remains unresolved.^[1e,5] Durbeej et al. did not find evidence for an orbital interaction between cob(II)alamin and intermediate radicals as proposed by Buckel et al.,^[1e] and there is no experimental evidence for this interaction. In a further computational study focusing on methylmalonyl-CoA mutase, Bucher et al.^[28] used Car-Parrinello molecular dynamics to explore the role of both 2'-OH and 3'-OH in stabilizing the Ado radical. They stated that the magnitude of the interaction of the 3'-OH with the C19-H was "somewhat less in the enzymatic environment than in the gas phase". The experimental results given in this paper show that this interaction must be significantly less than that previously calculated.

Experimental Section

General: Chemicals and deuterated solvents were obtained from reputable suppliers. Cyanocobalamin (CNCbl, vitamin B₁₂, **6**) was a generous gift from DSM Nutritional Products (Basel/Switzerland) and Professor Y. Murakami (Fukuoka, Japan). The chemicals were of reagent grade and used without further purification. Solutions used for reductions were sodium acetate (100 mM, pH 3), potassium phosphate (100 mM, pH 7.0), or potassium carbonate (pH 10.8). The pH of the samples was adjusted to other required values by using pH paper or a pH microelectrode before reduction. Because it was found that pH electrodes react with hydrogen and deuterium in a similar manner, the shift between pD and pH values was compensated for by adjusting the pH of the samples after dissolving the appropriate amount of buffer salts in the respective solvent, according to the standards given in the literature.^[31] Note that for reasons of simplicity, pH is used to describe the samples that were prepared in D₂O. All incubations under reducing conditions were done in an anaerobic chamber (5% H₂ in N₂). All reductions and reoxidations were monitored for completion by using UV/Vis spectroscopy. The samples were tempered at 20 °C in air; for incubations at 37 °C, a heating block was used.

Organic synthesis: Three adenine derivatives were prepared as chlorinated alkylating agents (Scheme 2). N⁶-Carbobenzoxyadenine (**8**) was synthesized as described.^[32] Methylbromoacetate was used to convert **8** to methyl N⁶-carbobenzoxy-2-(6-amino-9H-purin-9-yl)acetate (**9**),^[32] which was subsequently deprotected to form N⁶-carbobenzoxy-2-(6-amino-9H-purin-9-yl)acetic acid (**10**).^[33] Introduction of a chloroethyl group gave N⁶-carbobenzoxy-2-(6-amino-9H-purin-9-yl)-N-(2-chloroethyl)acetamide (**11**),^[34] and the subsequent Pd-catalyzed deprotection of the amine gave the first alkylating agent 2-(6-amino-9H-purin-9-yl)-N-(2-chloroethyl)acetamide (**12**).^[35] The second chlorinated adenine, 5-chloro-2',5'-dideoxyadenosine (**14**), was prepared from 2'-deoxyadenosine (**13**) according to published procedures with slight modifications.^[36] The third chlorinated adenine, 5-chloro-3',5'-dideoxyadenosine (**16**) was prepared similarly from 3'-deoxyadenosine (**15**). These three alkylating agents were used to generate alkylcobalamins from CNCbl (**6**) (Scheme 1) by using modified, published procedures.^[37] For the synthesis of (R)- and (S)-2,3-dihydroxypropylcobalamin (**R2**, **S2**), a previously published method,^[23a] in which CNCbl (**6**) was reacted with (R)- or (S)-1-chloropropane-2,3-diol (Scheme 1), was modified. For details of the organic synthesis and NMR spectra, see the Supporting Information (NMR data are found in Table S2). For UV/Vis characterisation of **1**, **3**, **4**, and **5**, see the Supporting Information (Figure S11; in addition, see ref. [38] for **3** and **4**).

Analytical methods: NMR spectra for HOCbl (**7**) and 5'-deoxyadenosylcobalamin (**1**) were recorded on Bruker AVANCE 300 B and AVANCE 600 spectrometers with 10 mg mL⁻¹ samples (standard 1D-¹H NMR and ¹H-¹H-DQF-COSY spectroscopy). NMR spectra for (R)- and (S)-2,3-dihydroxypropylcobalamin (**R2**, **S2**) (30 mg mL⁻¹ at 45 °C to increase solubility) were recorded on Jeol ECS-400 MHz (only for standard ¹H NMR spectroscopy) and Jeol Lambda 500 MHz machines (advanced measurements), including 2D NOESY (mixing times of 400 and 600 ms), 2D ROESY (spin-locking (mixing) times of 150 and 250 ms), double pulsed field gradient spin-echo 1D NOE and ROE experiments (mixing times of 500 and 750 ms)^[21] performed with selective excitation of the C19-H or of target protons of the 2,3-hydroxypropyl group, and field gradient HMBC experiments with timings optimized for long range couplings between ¹H and ¹³C of 2, 4, 6, or 8 Hz. NMR spectra of the samples (compounds **3–5** and **8–16**) for biochemical testing with glutamate mutase were recorded on a Bruker AV-500 spectrometer (Karlsruhe, Germany) and their data processing was carried out with ACD/SpecManager. The chemical shifts are given in ppm relative to the signal from the deuterated solvent. EPR measurements were recorded on a Bruker X-band EPR spectrometer EMX-6/1 with a rectangular standard cavity (77 K). The sample concentration was 10 mg mL⁻¹. After reduction, the samples were incubated for 3 h before being stored in liquid nitrogen.

The cobalamins (**3**, **4**, and **5**) that were intended for enzymatic assays with glutamate mutase were purified and analysed by HPLC and HPLC-

ESI-MS. HPLC solvents were 0.1% aqueous trifluoroacetic acid (A) and methanol (B). HPLC analyses were performed on a Merck-Hitachi L-7000 system that is equipped with a diode array UV/Vis spectrometer and Macherey–Nagel Nucleosil C-18ec RP columns (particle size: 5 μm; pore size: 100 Å; 250×3 mm; flow rate: 0.5 mL min⁻¹). Preparative HPLC separations were performed on a Varian Prostar system equipped with two Prostar 215 pumps, a Prostar 320 UV/Vis detector and Macherey–Nagel Nucleosil C-18ec RP columns (particle size: 7 μm; pore size: 100 Å; 250×40 mm; flow rate: 40 mL min⁻¹). HPLC-ESI-MS spectra were measured on a Bruker HCT spectrometer equipped with an Aquinity UPLC (Waters) by using Nucleosil C-18ec RP columns (particle size: 5 μm; pore size: 100 Å; 250×3 mm; flow rate: 0.3 mL min⁻¹). HPLC-ESI-MS solvents were 0.1% formic acid (A) and methanol (B). The following gradient (A) was used for all HPLC, HPLC-ESI-MS, and preparative HPLC measurements: 25% B for 5 min, then to 100% B over 25 min, then 100% B for 10 min. The following gradient (B) was used only for compound **4**: 10% B for 2 min, then to 100% B over 10 min, then 100% B for 13 min.

All MALDI-TOF-MS measurements of the deuterium exchange experiments were done on an Applied Biosystems 4800Plus MALDI-TOF/TOF mass spectrometer. The samples were measured directly upon being dissolved in water and after 6 h to check for a difference in exchange. α -Cyano-4-hydroxycinnamic acid in 50% acetonitrile (0.1% trifluoroacetic acid in H₂O) as a matrix was mixed in a dilution series (2-, 4-, 8-, 16-, 32-fold) for sample preparation. Sheffield ChemPuter (webpage retrieved on 1 February 2012: <http://winter.group.shef.ac.uk/chemputer/isotopes.html>) was used to generate theoretical values of natural-abundance isotopic distribution patterns for MALDI-TOF-MS. The Data Explorer from Applied Biosystems was used to process MALDI-TOF-MS data and extract integrals of individual signals. The monoisotopic signal of unlabeled cob(III)alamin without an upper ligand was used to calculate its whole isotopic distribution pattern (based on natural abundance and a reference measurement of unlabeled hydroxocobalamin; see the Supporting Information, Table S1). This was then subtracted from the signals with higher mass to reveal the pattern caused by +1 Da labeled cob(III)alamin, which, in turn, was subtracted from the remaining signal to reveal the +2 Da labeled cob(III)alamin. The ratio of the signals were calculated and given (in percent) relative to the total amount of cob(III)alamin before exchange. These values were corrected for errors (see the Supporting Information). All other mass spectra were recorded either in the positive or negative mode on an Esquire HCT from Bruker (Bremen, Germany).

Deuterium exchange of cobalamins under reducing conditions:

Cob(II)alamin reduction with dithiothreitol (DTT): Hydroxocobalamin (HOCbl, **7**, 10 mg mL⁻¹) was reduced by using DTT (0.1 M) in D₂O. The reoxidation was done by using potassium hexacyanoferrate(III) (0.2 M) in D₂O. For analysis, the samples were desalted on C18 columns (Sep-Pak Vac from Waters). The columns were conditioned with methanol, equilibrated with D₂O, loaded with solutions of the sample in D₂O, and then eluted with acetonitrile in D₂O (50%). The samples were freeze-dried and suspended in H₂O prior to MALDI-TOF-MS measurements. Initially, the samples were dissolved in D₂O and used for NMR spectroscopy, but no clear spectra could be obtained. Additional purification by using HPLC (RP18 reverse-phase semipreparative column, solution gradient of 0 to 80% acetonitrile in H₂O) or recrystallization from water/acetone (1:10) did not lead to sufficiently clear NMR spectra.

Cob(II)alamin reduction with PtO₂/H₂: Compound **7** (10 mg mL⁻¹) was stirred with PtO₂ (0.5 mg mL⁻¹) under a H₂/N₂ atmosphere (5%). For reoxidation, the catalyst was filtered off and the sample was incubated in air (10 h). No further purification for NMR analysis was needed. For MALDI-TOF-MS, the samples were freeze-dried and dissolved in H₂O.

Cob(II)alamin generation by photolysis: 5'-Deoxyadenosylcobalamin (**1**, 10 mg mL⁻¹) in D₂O was irradiated for 6 h (120 W incandescent light bulb) for three successive days in an NMR tube in an anaerobic chamber. The control sample was kept in the dark under air. After reoxidation in air (10 h), no further purification was done for NMR analysis and MALDI-TOF-MS.

Cob(I)alamin: Compound **7** (10 mg mL⁻¹) was reduced by using sodium dithionite (1 M) in D₂O.^[22] The samples were reoxidized in air (10 h) and purified on a C18 column (see details above). For kinetic studies monitored by MALDI-TOF-MS, the samples were first reoxidized with a slight excess of potassium hexacyanoferrate(III). The samples were freeze-dried and redissolved in H₂O for MALDI-TOF-MS. For NMR spectroscopy, the samples were recrystallized from water/acetone (1:10). The NMR samples in D₂O were adjusted to pH 9 with a pH microelectrode.

X-ray crystal-structure determination: X-ray crystallographic data were collected on an Oxford Diffraction Gemini A Ultra diffractometer at 150 K by using Cu K α radiation ($\lambda = 1.54184$ Å). Analytical numeric absorption corrections that use a multifaceted crystal model which is based on expressions derived by R. C. Clark and J. S. Reid^[59] were applied, based on symmetry-equivalent and repeated reflections. Structures were solved by direct methods and refined on all unique F^2 values, with anisotropic non-H atoms and constrained riding isotropic H atoms. High anisotropy of some atoms in solvent acetone molecules, which are present in the crystal structure of **R2b**, indicate disorder, but this could not be resolved satisfactorily by split positions and has been ignored. Disordered water molecules that could not be modeled as discrete atoms in **R2b** and **S2b** were treated by the SQUEEZE procedure of PLATON.^[40] Programs used were CrysAlisPro for data collection, integration, and absorption corrections,^[41] and OLEX2^[42] or SHELXTL^[43] for structure solution, refinement, and graphics. Full details about crystallographic experimental information is provided in the Supporting Information, together with a list of bond lengths and angles. CCDC-864775 (**R2b**) and 864776 (**S2b**) contain the supplementary crystallographic data for this paper. These data can be obtained free of charge from The Cambridge Crystallographic Data Centre via www.ccdc.cam.ac.uk/data_request/cif.

Enzymatic purification and assays for glutamate mutase kinetic studies:

Glutamate mutase (components S and E) from *Clostridium cochlearium* was recombinantly produced and purified by following published procedures.^[11a] Methylaspartase was purified from cell-free extracts of *Clostridium tetanomorphum*.^[44] The components S and E were assembled into the holoenzyme in the presence of **1** or **3**, **4**, and **5**. A standard coupled enzyme assay with methylaspartase was used for the measurement of glutamate mutase kinetic parameters (37°C, 50 mM Tris, pH 8.3, 0.05 mM mercaptoethanol). The assays for enzymatic activity were performed by using component E (GlmE) and a 14-fold excess of component S (GlmS) together with the cofactor analogue at varying concentrations. All alkylcobalamins (**1**, **3**, **4**, and **5**) were shielded from light and measurements were performed under a protective red light. The initial specific activities of the partially purified enzymes were: methylaspartase (44 U mg⁻¹), GlmS (66 U mg⁻¹), and GlmE (18 U mg⁻¹). The specific activity of GlmS was determined by using an excess of GlmE, and vice versa. When measuring K_M and V_{max} for 5'-deoxyadenosylcobalamin (**1**), GlmS (5 μg), GlmE (2.6 μg), methylaspartase (36 μg), and glutamic acid (20 mM) were used, and the cofactor concentration was varied (0.32 μM–25 μM). In the case of cobalamin derivatives **3**, **4**, and **5**, ten times the amount of apoglutamate mutase was used. 3',5'-Dideoxyadenosylcobalamin (**4**) concentrations were varied between 0.35 μM and 70 μM. The concentration of component E was used to calculate k_{cat} for compounds **1** and **4**. After mixing all ingredients together, the cuvette was incubated for 5 min at 37°C to ensure the formation of the holoenzyme composed of E, S, and either **1** or one of the analogues **3**, **4**, or **5**. Then the reaction was started with (S)-glutamate, and the formation of (2S,3S)-methylaspartate was measured continuously at 240 nm by conversion to mesaconate by using mesaconase as an auxiliary enzyme. In this assay, the inclusion of **1** or the analogue had two different functions: the assembly of the holoenzyme, and the action as a cofactor for catalysis.

Acknowledgements

We are indebted to Professor Christoph Kratky, Graz, Austria for providing the crystal structure presented in Figure 5. We thank the German Re-

search Foundation (W.B. and B.T.G.), the EPSRC (B.T.G. and W.M.) and the Fonds der chemischen Industrie (W.B.) for generous financial support. We thank Dr. Antonio Pierik for EPR spectra, Jörg Kahnt for MALDI-TOF-MS, Dr. Ronald Wagner and Dr. Xiulan Xie for NMR (all from Marburg, Germany), and Dr. Karel Zelenka (Zürich) for the synthesis of compounds **3** and **4**.

- [1] a) J. Halpern, *Science* **1985**, *227*, 869–875; b) R. Banerjee, *Chemistry and Biochemistry of B₁₂*, Wiley, New York, **1999**; c) E. N. G. Marsh, C. L. Drennan, *Curr. Opin. Chem. Biol.* **2001**, *5*, 499–505; d) K. L. Brown, *Chem. Rev.* **2005**, *105*, 2075–2150; e) W. Buckel, C. Kratky, B. T. Golding, *Chem. Eur. J.* **2006**, *12*, 352–362; f) E. N. G. Marsh, D. P. Patterson, L. Li, *ChemBioChem* **2010**, *11*, 604–621; g) K. Gruber, B. Puffer, B. Kräutler, *Chem. Soc. Rev.* **2011**, *40*, 4346–4363; h) W. Buckel, B. T. Golding, *Radical Enzymes. Encyclopedia of Radicals in Chemistry, Biology and Materials*, Wiley, New York, **2012**.
- [2] P. Nordlund, P. Reichard, *Annu. Rev. Biochem.* **2006**, *75*, 681–706.
- [3] a) B. P. Hay, R. G. Finke, *J. Am. Chem. Soc.* **1986**, *108*, 4820–4829; b) B. P. Hay, R. G. Finke, *J. Am. Chem. Soc.* **1987**, *109*, 8012–8018.
- [4] a) R. Banerjee, *Chem. Rev.* **2003**, *103*, 2083–2094; b) T. Toraya, *Chem. Rev.* **2003**, *103*, 2095–2127.
- [5] P. Kozłowski, T. Kamachi, T. Toraya, K. Yoshizawa, *Angew. Chem.* **2007**, *119*, 998–1001; *Angew. Chem. Int. Ed.* **2007**, *46*, 980–983.
- [6] B. T. Golding, L. Radom, *J. Am. Chem. Soc.* **1976**, *98*, 6331–6338.
- [7] a) C. Raynaud, P. Sarçabal, I. Meynial-Salles, C. Croux, P. Soucaille, *Proc. Natl. Acad. Sci. USA* **2003**, *100*, 5010–5015; b) J. R. O'Brien, C. Raynaud, C. Croux, L. Girbal, P. Soucaille, W. N. Lanzilotta, *Biochemistry* **2004**, *43*, 4635–4645.
- [8] a) V. Bandarian, G. H. Reed, *Biochemistry* **2002**, *41*, 8580–8588; b) S. C. Ke, *Biochim. Biophys. Acta Gen. Subj.* **2003**, *1620*, 267–272; c) J. M. Canfield, K. Warncke, *J. Phys. Chem. B* **2005**, *109*, 3053–3064; d) L. Sun, O. A. Groover, J. M. Canfield, K. Warncke, *Biochemistry* **2008**, *47*, 5523–5535.
- [9] N. Shibata, H. Tamagaki, N. Hieda, K. Akita, H. Komori, Y. Shomura, S. Terawaki, K. Mori, N. Yasuoka, Y. Higuchi, T. Toraya, *J. Biol. Chem.* **2010**, *285*, 26484–26493.
- [10] N. Shibata, Y. Nakanishi, M. Fukuoka, M. Yamanishi, N. Yasuoka, T. Toraya, *J. Biol. Chem.* **2003**, *278*, 22717–22725.
- [11] a) O. Zelder, B. Beatrix, U. Leutbecher, W. Buckel, *Eur. J. Biochem.* **1994**, *226*, 577–585; b) H. Bothe, D. J. Darley, S. P. J. Albracht, G. J. Gerfen, B. T. Golding, W. Buckel, *Biochemistry* **1998**, *37*, 4105–4113; c) G. H. Reed, S. O. Mansoorabadi, *Curr. Opin. Struct. Biol.* **2003**, *13*, 716–721; d) S. O. Mansoorabadi, R. Padmakumar, N. Fazliddinova, M. Vlasie, R. Banerjee, G. H. Reed, *Biochemistry* **2005**, *44*, 3153–3158.
- [12] a) F. Mancia, N. H. Keep, A. Nakagawa, P. F. Leadlay, S. McSweeney, B. Rasmussen, P. Bösecke, O. Diat, P. R. Evans, *Structure* **1996**, *4*, 339–350; b) K. Gruber, R. Reitzer, C. Kratky, *Angew. Chem.* **2001**, *113*, 3481–3484; *Angew. Chem. Int. Ed.* **2001**, *40*, 3377–3380.
- [13] A. M. Calafat, L. G. Marzilli, *J. Am. Chem. Soc.* **1993**, *115*, 9182–9190.
- [14] B. Durbeej, G. M. Sandala, D. Bucher, D. M. Smith, L. Radom, *Chem. Eur. J.* **2009**, *15*, 8578–8585.
- [15] C. A. Hunter, *Angew. Chem.* **2004**, *116*, 5424–5439; *Angew. Chem. Int. Ed.* **2004**, *43*, 5310–5324.
- [16] a) E. A. Guggenheim, *Mixtures: The Theory of the Equilibrium Properties of Some Simple Classes of Mixtures, Solutions and Alloys*, Clarendon Press, Oxford, **1952**; b) R. D. Green, *Hydrogen Bonding by C–H Groups*, Macmillan, London, **1974**.
- [17] a) A. Kolocouris, *J. Org. Chem.* **2009**, *74*, 1842–1849; b) S. Horowitz, J. D. Yesselman, H. M. Al-Hashimi, R. C. Trievel, *J. Biol. Chem.* **2011**, *286*, 18658–18663.
- [18] D. A. Boudreaux, J. Chaney, T. K. Maiti, C. Das, *FEBS J.* **2012**, *279*, 1106–1118.
- [19] R. J. Anderson, R. M. Dixon, B. T. Golding, *J. Organomet. Chem.* **1992**, *437*, 227–237.
- [20] N. W. Alcock, R. M. Dixon, B. T. Golding, *J. Chem. Soc. Chem. Commun.* **1985**, 603–605.
- [21] a) K. Stott, J. Keeler, Q. N. Van, A. J. Shaka, *J. Magn. Reson.* **1997**, *125*, 302–324; b) W. Bauer, A. Soi, A. Hirsch, *Magn. Reson. Chem.* **2000**, *38*, 500–503.
- [22] J. M. Pratt, in *Inorganic Chemistry of Vitamin B₁₂*, Academic Press, New York, **1972**, p. 201.
- [23] a) R. M. Dixon, B. T. Golding, O. W. Howarth, J. L. Murphy, *J. Chem. Soc. Chem. Commun.* **1983**, 243–245; b) K. Kurumaya, M. Kajiwara, *Chem. Pharm. Bull.* **1989**, *37*, 9–12.
- [24] a) R. Bonnett, D. G. Redman, *Proc. R. Soc. Lond. A* **1965**, 288, 342–343; b) H. A. O. Hill, B. E. Mann, J. M. Pratt, R. J. P. Williams, *J. Chem. Soc. A* **1968**, 564–567; c) S. A. Cockle, H. A. O. Hill, R. J. P. Williams, B. E. Mann, J. M. Pratt, *Biochim. Biophys. Acta Gen. Subj.* **1970**, *215*, 415–418.
- [25] S. Scheiner, *Phys. Chem. Chem. Phys.* **2011**, *13*, 13860–13872.
- [26] D. Lexa, J. M. Saveant, *Acc. Chem. Res.* **1983**, *16*, 235–243.
- [27] a) E. A. Symons, M. J. Clermont, *J. Am. Chem. Soc.* **1981**, *103*, 3127–3130; b) I. F. Tupitsyn, A. S. Popov, *Russ. J. Gen. Chem.* **2001**, *71*, 89–101.
- [28] D. Bucher, G. M. Sandala, B. Durbeej, L. Radom, D. M. Smith, *J. Am. Chem. Soc.* **2012**, *134*, 1591–1599.
- [29] a) K. P. Jensen, U. Ryde, *J. Am. Chem. Soc.* **2005**, *127*, 9117–9128; b) J. B. Rommel, J. Kästner, *J. Am. Chem. Soc.* **2011**, *133*, 10195–10203.
- [30] A. M. Calafat, S. Taoka, J. M. Puckett, C. Semerad, H. Yan, L. Luo, H. Chen, R. Banerjee, L. G. Marzilli, *Biochemistry* **1995**, *34*, 14125–14130.
- [31] a) R. Gary, R. G. Bates, R. A. Robinson, *J. Phys. Chem.* **1964**, *68*, 3806–3809; b) M. Paabo, R. G. Bates, *Anal. Chem.* **1969**, *41*, 283–285.
- [32] S. A. Thomson, J. A. Josey, R. Cadilla, M. D. Gaul, C. F. Hassman, M. J. Luzzio, A. J. Pipe, K. L. Reed, D. J. Ricca, R. W. Wiethe, S. A. Noble, *Tetrahedron* **1995**, *51*, 6179–6194.
- [33] K. L. Dueholm, M. Egholm, C. Behrens, L. Christensen, H. F. Hansen, T. Vulpius, K. H. Petersen, R. H. Berg, P. E. Nielsen, O. Buchardt, *J. Org. Chem.* **1994**, *59*, 5767–5773.
- [34] K. Zhou, F. Zelder, *Angew. Chem.* **2010**, *122*, 5305–5307; *Angew. Chem. Int. Ed.* **2010**, *49*, 5178–5180.
- [35] G. M. Anantharamaiah, K. M. Sivanandaiah, *J. Chem. Soc. Perkin Trans. 1* **1977**, 490–491.
- [36] a) D. W. Jacobsen, R. J. Holland, Y. Montejano, F. M. Huenekens, *J. Inorg. Biochem.* **1979**, *10*, 53–65; b) K. L. Brown, S. Cheng, X. Zou, J. Li, G. Chen, E. J. Valente, J. D. Zubkowski, H. M. Marques, *Biochemistry* **1998**, *37*, 9704–9715.
- [37] a) B. Zagalak, J. Pawelkiewicz, *Acta Biochim. Pol.* **1965**, *12*, 219–228; b) S. Gschösser, R. B. Hannak, R. Konrat, K. Gruber, C. Mikl, C. Kratky, B. Kräutler, *Chem. Eur. J.* **2005**, *11*, 81–93.
- [38] a) M. Ichikawa, T. Toraya, *Biochim. Biophys. Acta Protein Struct. Mol. Enzymol.* **1988**, *952*, 191–200; b) M. P. Jensen, J. Halpern, *J. Am. Chem. Soc.* **1999**, *121*, 2181–2192.
- [39] R. C. Clark, *Acta Crystallogr. Sect. A* **1995**, *51*, 887–897.
- [40] a) A. L. Spek, *J. Appl. Crystallogr.* **2003**, *36*, 7–13; b) A. L. Spek, *Acta Crystallogr., Sect. D: Biol. Crystallogr.* **2009**, *65*, 148–155.
- [41] CrysAlisPro, Version 1.171.35 ed., Agilent Technologies, **2010**, Xcalibur CCD system.
- [42] O. V. Dolomanov, L. J. Bourhis, R. J. Gildea, J. A. K. Howard, H. Puschmann, *J. Appl. Crystallogr.* **2009**, *42*, 339.
- [43] G. M. Sheldrick, *Acta Crystallogr. Sect. A* **2008**, *64*, 112.
- [44] H. A. Barker, R. D. Smyth, H. J. Bright, L. L. Ingraham, *Methods Enzymol.* **1962**, *5*, 827–832.

Received: May 25, 2012

Revised: August 21, 2012

Published online: October 18, 2012